A Novel Architecture for Ultra-High Signal-to-Interference-Noise-Ratio Reception in Visible Light Communication

MD Rashed Rahman, S M Towhidul Islam, Ashwin Ashok
Department of Computer Science, Georgia State University
{mrahman19,sislam9}@student.gsu.edu, aashok@gsu.edu

***Abstract*—Theoretical models estimate visible light communication (VLC) data capacity to be of the order of Tera-bits-per-second (Tbps). However, practical limitations in receiver designs have limited state-of-the-art VLC prototypes to (multiple) orders of magnitude lower data rates. This paper explores a new architecture to realize ultra-high data rates in visible light communication systems by dramatically improving the Signal-to-Interference-Noise-Ratio (SINR) at the receiver. The key idea is to leverage the fast sampling rates of photodiode receivers and integrate a shutter mechanism that filters noise and interference thus creating a high-speed imaging receiver effect. Through adaptive selection of the exact receiver area over which the transmitted light is detected, the SINR can be dramatically increased yet not compromising the high sampling rate achievable using state-of-the-art photoreceptors. In addition to introducing the new hybrid architecture for high SINR reception, in this paper, we study the feasibility of noise and interference reduction through a proof-of-concept experimentation.**

I. INTRODUCTION

The significant growth in the wireless data traffic has initiated the need for expanding the range of frequencies used for wireless data communication. This has opened up new opportunities for utilizing the unused bands of the electromagnetic spectrum such as optical frequencies for wireless data communication through the Visible Light Communication (VLC) technology [1], [2]. VLC is a wireless communication technology that operates unregulated in the visible–light band (400–800 THz frequencies or 380–780 nm wavelengths) of the electromagnetic spectrum, and is enabled by light emitting elements such as light emitting diodes (LED) and light receiving elements such as photodiodes (PD).

The semiconductor properties of LEDs and PDs enable them to be switched at extremely high rates thus allowing transmission/reception of light beams at extremely high frequencies. VLC is a line–of–sight (LOS) technology, which means it requires the light transmitter and receiver to be within the distance and angular range (field–of–view (FOV)) of one another. The LOS requirement enables efficient space reuse allowing spatial–multiplexing of VLC links between multiple transmitters and receivers. The availability of a huge unrestricted visible–light spectrum and the spatio–temporal qualities makes VLC a strong proponent for high–speed wireless communication.

Over the past few years, VLC technology has garnered significant interest in both academic and industrial fronts. Research and development in VLC has exemplified VLC applications across diverse areas including smart sensing for human–computer interaction [3], precise indoor localization [4], inter–vehicular and vehicular to infrastructure communication [5] and underwater communication [6]. Operating over an unrestricted 400THz of bandwidth, VLC is capable of extremely high data rate communication, of the order of Gbps and beyond. VLC channel studies [7] estimate its data capacity to the order of Tbps. However, in practice, VLC systems are still operating in the range of Kbps–Mbps. The IEEE 802.15.7 [8] standard is being developed in recognition of the VLC technology and claims to support data rates upto 96Mbps. The commercialized LiFi [9] system currently supports upto 40Mbps. However, even with such rapid advancements in the technology, the state–of–the art data rates in VLC is dramatically less than its actual wireless data capacity. Clearly, there is a large gap to fill to reach ultra–high speeds.

Achieving ultra–high data rates in VLC close to its wireless data capacity is the key vision of our research. With the increasing density of interconnected devices/machines and the interaction among them, the number of bits–per–second required for data communication per unit geographical area has significantly increased. We exemplify this through a motivational example:

Motivational scenario: Virtual Reality (VR) headsets, that are available off–the–shelf today, are tethered to a device that can act as a local computing server, due to their limited computing power on the wearable device. The server processes, renders and communicates the video frames to the headset, where it gets displayed onto the user's view. To avoid motion–blur and disorientation to the user, and thus provide an immersive experience to the user, it is estimated [10], for each eye, the video frames must be of atleast 4K Ultra–High Definition (UHD) quality (8.3Mpixels) and rendered at a minimum of 90 frames–per–second (FPS). Considering video frames are in RGB color format at 24 pixel depth (8 bits per R–G–B channel) the data rate requirement for the tethering link is over 20Gbps per headset. For a dense use–case scenario involving multiple headsets (e.g. museum attendees, gaming

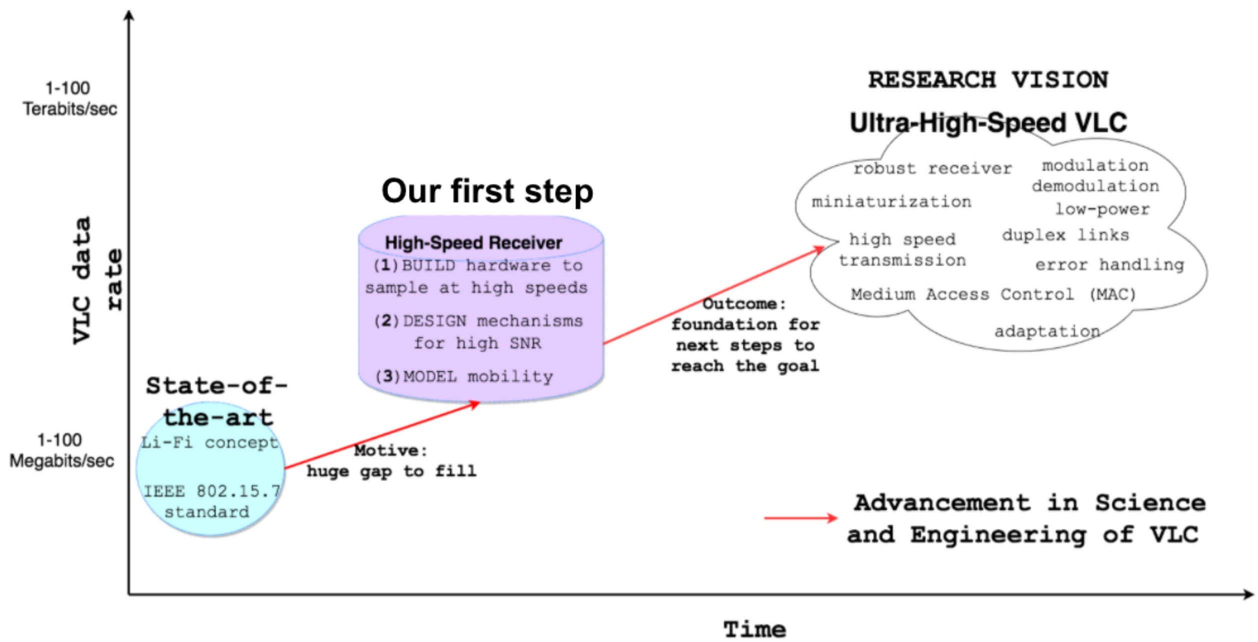

Fig. 1: Research vision for High–Speed VLC

convention, classroom teaching), the bandwidth requirement is of the order of few 100s—1000s of GHz, which is much beyond the bandwidth capacity of today's and next generation radio wireless standards [11].

Considering the insufficiency of bandwidths in today's wireless technologies, *achieving ultra–high–speed VLC is not only an opportunity but also is a necessity*. Achieving data rates close to capacity in VLC requires significant advancements in science and engineering of highly efficient and robust VLC architectures.The fundamental issue with traditional VLC architectures is that, photodiodes can sample light signals at extremely high rates but signal quality suffers under high ambient noise scenarios. Multiple–input Multiple–Output (MIMO) through photodiode arrays and imaging receivers can spatially isolate noisy pixels due to the definite array structure, however, are extremely limited in sampling rates. Such architectural differences create a data–rate versus signal quality trade off in VLC. In this paper, we present a new VLC architecture to overcome this trade off and achieve high signal quality reception through a hybrid design that can leverage the advantage of photodiodes to achieve high data rates and the noise isolation opportunity from imaging sensors.

We propose to combine the fast sampling nature of photodiodes and the noise isolation property of imaging array structures into a unified structure that will *emulate a high–speed image sensing receiver*. Through this unified design the receiver will be able to select the exact area over which the transmitted signal is detected on the array, and thus isolate signal from noise and other interfering optical sources. In this way, the SINR can be dramatically increased yet not compromising the high sampling rates of the photodetector. The isolation property of the receiver also allows for incorporating light tracking techniques to identify the exact location (on the array) of the detected transmitter signal.

At a conceptual level, we illustrate our research vision for advancing the high-speed VLC technology through the chart in Fig. 1. As a first step in achieving high-speed VLC designs, we make the following contributions in this paper:

1) We introduce a hybrid receiver architecture design for VLC that combines benefits of photodiode and imaging receivers.
2) We conduct experimental studies to verify the feasibility of SINR enhancement through noise and interference elimination using our proof–of–concept prototype hardware setup.

II. Related Work

We will review state–of–the–art developments in achieving high speed VLC. In addition, we will also review some of the new application dimensions in VLC to give an idea as to how the technology is diversifying as a promising wireless technology.

LiFi. The state–of–the–art in commercialized VLC technology is the LiFi–X system [9]. LiFi–X includes a modified LED light bulb transmitter and a receiver hardware dongle with USB support that connects to a PC. LiFi–X is capable of 40Mbps uplink and downlink duplex VLC using a white LED transmitter and a high power, high–cost avalanche photodiode receiver. However, spatial scaling, i.e. adding an extra photodiode in this receiver, can be extremely challenging due to the form–factor limitations, driving amplifier load, and the firmware overhead for processing an additional receiver element.

IEEE 802.15.7 standard. While the IEEE VLC standard theoretically supports data rates upto 96Mbps [8], the simulation studies in the draft revision to the standard, IEEE 802.15.7r1 [12], claim Gbps data rates capability using orthogonal frequency division multiplexing (OFDM) [13] modulation. OFDM requires knowledge of the channel parameters to allot sub–channels for multiplexing, and this is proposed to be achieved by channel estimation using feedback loops. The practical viability and reliability of such designs can be extremely challenging considering scale and mobility.

Multiple–Input Multiple–Output (MIMO). The concept of MIMO, using arrays of LEDs and photoreceptors, has gained prominence in VLC architecture design. Using array transmitters and receivers allows for scaling the the data rate by the multiplexing data communication across multiple LED–photoreceptor channels. Multiple array elements also increases the field–of–view of the receiver thus allowing for some mobility within LOS. Array photoreceptors can be either a set of photodiodes arranged in a specific fashion or correspond to a set of pixel elements of an image sensor. The challenge with photodiode arrays is that they allow more *noise*, from ambient light (sunlight and artificial lighting), into the receiver due to the wide field–of–view, thus affecting received signal quality and data rate. To account for this it requires very high amplification and noise reduction which can be complex and costly [14]. Image sensors can help isolate the noise because of its spatial structure, however, are extremely limited in sampling rates or frame–rates. Even the fastest image sensors can sample only at the order of 1000 FPS [15], which is orders of magnitude less than that of a single photodiode ($10^6 - 10^9$ samples/second).

Free–space optics inspired. Recent work in fiber–wireless–fiber based architectures in free–space optics design, estimate data rates of the order of 10s to 100s of Gbps [16]. These systems use high power and high cost elements such as Laser diodes controlled by optical–fiber elements at the transmitter/receiver. These systems require bulky spatial light modulators (SLM) to direct the laser beam using mechanical steering to cover a wide angular range, if not, use high–cost avalanche photodiodes [17] at the receiver [14]. Due to the high cost, high power and complex hardware design, such architectures may not be appropriate for generic mobile VLC systems.

Camera Communication The ubiquity of high–resolution displays has generated significant interest in *screen–to–camera* communication where multiplexing using the large array of display pixels (LCD or LED) and camera pixels could scale data rates. The body of work in this space includes, PixNet [18], COBRA [19], HiLight [20], INFRAME++ [21], Styrofoam [22], LightSync [23] and Strata [24]. Even with the MIMO structure, the data rates achieved by these systems are limited to few Kbps for ranges of within 1–2 meters. These designs use specific encoding and receiver processing techniques to address visual distortions in the camera channel, and have very specific use–cases or work under only specific hardware configurations and/or ambient lighting conditions.

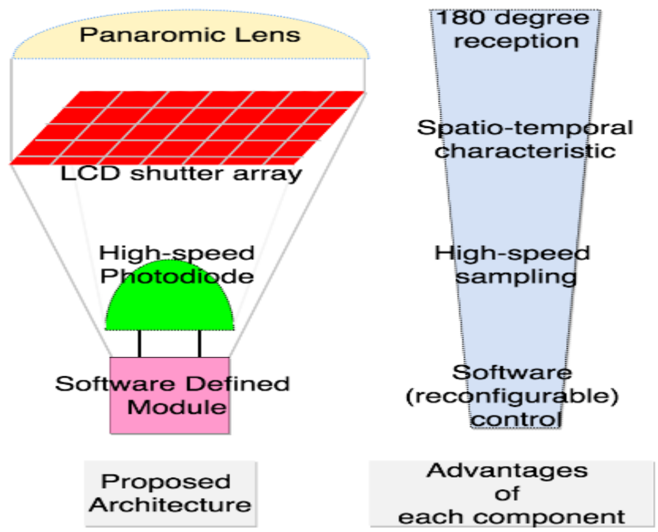

Fig. 2: Proposed Hybrid VLC Architecture

The Smart Lighting Research Center [25] at Boston University identifies the design of fast–switching and power–efficient LEDs for smart space solutions as one of its key research thrusts. Other thrusts include, LED–to–LED communication [26], power–line VLC networks [27], duplex VLC [28], backscatter VLC [29]. The survey paper [30] presents a consolidated list of existing VLC systems and the challenges in the domain from a scientific research perspective. The survey paper [31] discusses the challenges from a standardization and commercialization perspective. These efforts discuss and promote the diverse use–cases of VLC. However, there is a consensus that high data rate VLC system design is a need of the day.

III. Architecture

We combine the advantages of photodiodes and image sensors, and propose a novel receiver architecture that *emulates the functionality of image sensor arrays using a single photodiode*. The core idea of this design is to utilize the high–speed sampling of a photodetector and augment features of a typical image sensing array. We provide a conceptual overview of the architecture in Fig. 2.

The key components of the proposed design are the high–speed photodiode, a shutter mechanism, the computing unit and a panoramic lens. The shutter mechanism enables to spatially filter the noise and interference from the actual optical signal from the light source. In this regard, we use an off–the–shelf liquid–crystal–device (LCD) shutter array [32], where each element of the LCD array, or *pixel*, doubles up as a digital shutter based on the input voltage. Depending on the input voltage, the liquid crystals occupy a certain polarity thus allowing light to traverse through the pixel only if the polarity matches that of the incoming light beam, if not blocks the same. The receiver uses this functionality to

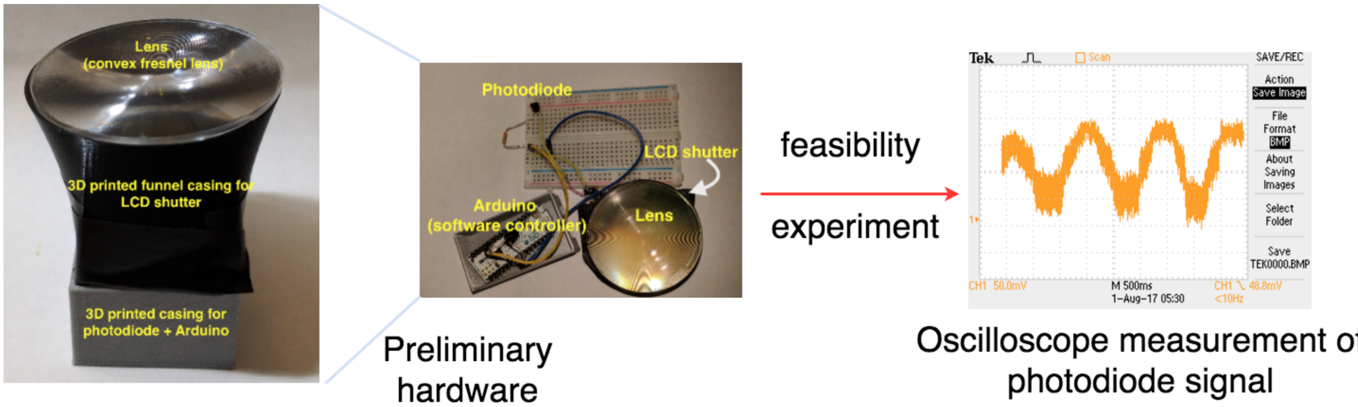

Fig. 3: Preliminary feasibility experiment setup.

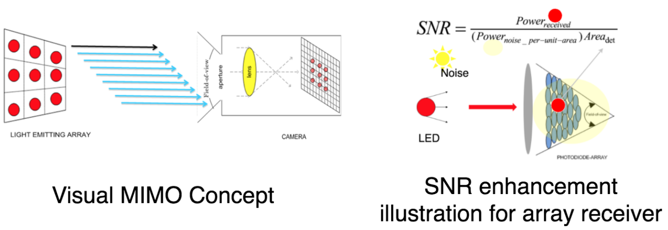

Fig. 4: Illustration of Signal–to–Noise–Ratio in array receiver. Visual MIMO figure adapted from [7]

control which light beam must be processed and what must be eliminated by the photodiode. The computing unit enables high sampling rate processing and hosting a software stack to incorporate control and other processing mechanisms. A typical software defined radio (SDR) unit, such as an Universal Software Radio Peripheral (USRP) [33] or an FPGA device, can serve as the computing unit. A panoramic lens fit to the Photodiode–LCD array will provide a wide–angle (180 degree) FOV to the receiver. The LCD array with the lens expands the effective FOV of the photodiode yet preserving its high sampling rate and eliminates the need for multiple photodiodes to achieve the array structure. The LCD array and photodiode are controlled independently using the computing unit. Such a modulo hardware architecture makes this design reconfigurable.

A. *Feasibility Tests*

The strength of the proposed hybrid architecture lies on two fundamental notions, that, (a) light sampling can be controlled using a digital shuttering mechanism, and (b) unwanted optical signals can be eliminated by separating signal from noise and interference directly in spatial domain.

To verify our notion (a), we conducted an experiment to test the feasibility of controlling light beam receptions using off–the–shelf photodiode–LCD shutter combinations. We developed a prototype of a LCD–integrated photodiode based optical detector (see Fig. 3), where we reused the LCD of an off–the–shelf 3D glasses and integrated it with an off–the–shelf photodiode [34] using an Arduino [35] microcontroller. The contraption was placed on a table pointing to the ceiling in an indoor office environment with artificial white lighting. The LCD was switched at 2Hz in an ON–OFF pattern and the photodiode set in an always–ON mode. The raw signal from the photodiode was recorded on an oscilloscope. The signal plot in Fig. 3 shows a signal wave approximately at 2Hz (500ms time period) and confirms our feasibility verification.

The basis for notion (b) is from our learnings from the visual MIMO model [7]. From a conceptual view, the Photodiode–LCD array can be viewed as a *single–element camera with extremely high frame rate*. We understand from Shannon Capacity formulation for communication that the throughput is logarithmic function of the SINR at the receiver. We use this fact and aim to improve the receiver SINR significantly such that it results in a steep increase in throughput. As illustrated in the conceptual diagram in Fig. 4, we set forth to improve SINR by first sampling the optical signal only over an area where it actually registers on the receiver array. This way, the effective area over which ambient optical noise accumulates is significantly reduced. In addition, such a spatial filtering enables eliminating interference from other sources. This way, if the noise–power (denominator) in SINR is made negligible, it results in a dramatic increase in the SINR value and thus improving demodulation and decoding efficiency at the receiver.

In the rest of this paper, we study the noise and interference elimination property of our proposed design through actual physical optical measurements and using SINR as the evaluation metric.

IV. General Experiment Setup

The key aspect of the work in this paper is the measurement study to cancel noise and interference through our novel VLC receiver. To this end, we arranged a measurement setup on an optical table to quantify the signal, noise and interference in an LED-to-Photodiode link. We ensured there are no vibrations or any movement that can impact the quality of our measurements. The measurements were conducted indoor, in an academic lab setting with sufficient indoor white lighting from the ceiling. The ambient lighting also includes the

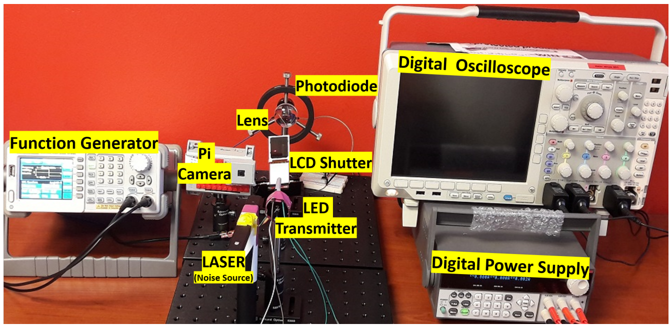

Fig. 5: General experiment setup.

sunlight from across the room through the glass window. The experiment was conducted on the less bright side of the room at a distance of 7m from the glass window. The LED-Photodiode link was setup such that it was at a right angle to the light reception from the glass window.

The general experiment setup is shown in Fig. 5, and consists of an off–the–shelf PIN photodiode [34], a red LED [36], a laser LED (acting as noise source) [37], an TFT LCD shutter [38]. We used a Keithley 2231A-30-3 digital power supply to power our LEDs [39] and a Tektronix digital oscilloscope [40] to monitor the output from the photodiode. We also used a digital multimeter to record the photodiode output voltage and current. We setup a RaspberryPi camera [41] on a plane parallel but translated from the LCD shutter center for visual verification.

To ensure the photodiode signals are registered on the multimeter and the scope, we amplified the photodiode output using a LM358N operational amplifier [42]. We used the circuit in non–inverting mode with a resistance of $R = 510k\Omega$ and the voltage output $V_o = RI_{pd}$, where I_{pd} was the received photocurrent. In the setup, we used an off–the–shelf aspheric condenser lens [43] to focus the light wave onto the photodiode. The focal length of the lens is 27mm and the photodiode was placed at the focal point of the lens in our experiment. The lens was placed behind the shutter covering the area of the shutter. The distance between the lens (shutter) and the photodiode is 2.7cm (focal length of the lens) and the distance between the shutter and LED transmitter is 16cm.

Fig. 6 shows a closeup view of our experiment setups. We setup two modes for our experiments, (a) closed box, where we covered the setup using a cardboard box to create a dark-room type environment by blocking the ambient light, and (b) open box, where we let the top part of the box open while one of the sides was covered with cardboard to block the sunlight from the glass window. In our experiments we physically blocked the sunlight and hence the ambient noise in our experiments is primarily from the ceiling white lights. As you can observe from the setup figures, we used a LASER LED and another RED LED light source which played the role of interfering (noise) sources for the primarily LED-Photodiode link.

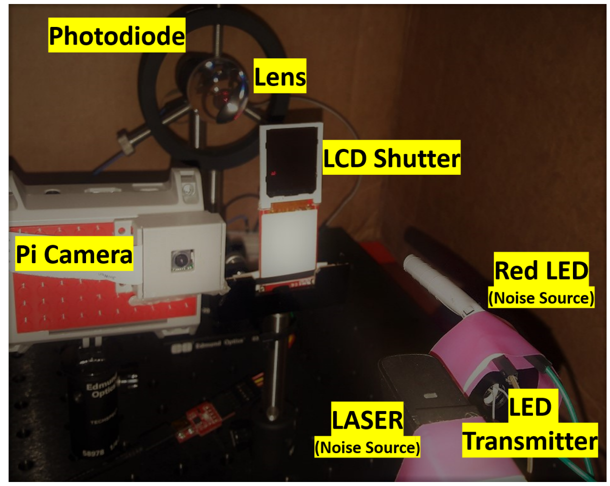

(a) Closed box experiment setup. We used the camera flash light to register the picture in the darkness of the closed box setup.

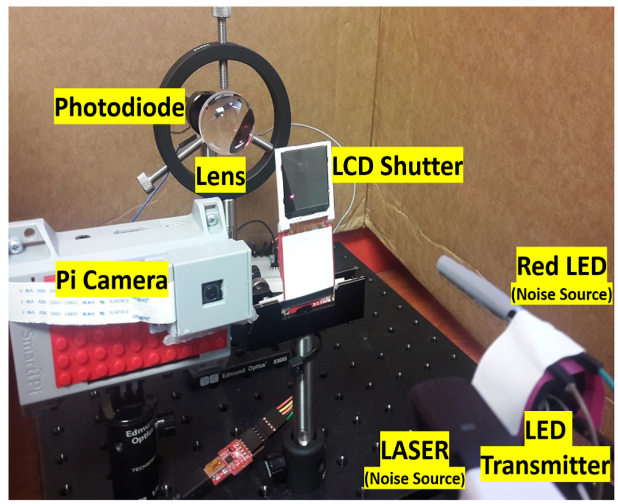

(b) Open box experiment setup

Fig. 6: Our measurement setups for (a) closed box testing and (b) open box testing

V. Spatial Noise Filtering

Using the setup shown in Fig. 6 (a), we conducted an experiment to measure the $SINR$ for different choices of reception area on the LCD shutter. We conducted the experiment in a closed–box setting to ensure no ambient lighting impacted the noise measurement. Hence, the noise measured in this experiment corresponds to the limited ambient lighting within the box (negligible) and the noise from the signal (typically very low). The main goal of this experiment is to understand the relative $SINR$ improvements if the area of the reception was centered around the area of the photodiode.

The experiment involved setting an LED in an always ON mode and directing at zero degree angle towards the shutter-lens-photodiode receiver setup. The LED transmitted 1mW of optical power. We measured the received noise signal voltage on the photodiode with the LED in OFF mode, as V_n, and the LED signal voltage as V_r when the LED was ON. Since there

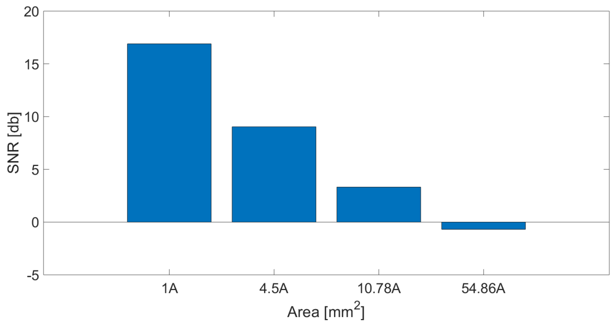

Fig. 7: SNR versus selected area of reception. SNR [db] $= 10log_{10}(SNR)$. Here A = 57.40mm^2. Resolution of LCD shutter = 240 x 320 pixels. Side length of the LCD shutter pixel = 0.2mm.

is no interference signal in this experiment, the SINR becomes the signal-to-noise-ratio (SNR). We compute the SNR as,

$$SNR = \frac{V_r^2 - V_n^2}{V_n^2} \tag{1}$$

We conducted the signal measurements for different values of area-of-shutter opening. We replaced the shutter shown in Fig. 5 with an identical model but larger resolution LCD shutter to ensure testing across a wide range of area selections. For each area selection we open the appropriate number of pixels considering it as a square region. Consider A = 57.40mm^2, we conducted these measurements for four area selections:

(i) 1A: Only the area corresponding to the actual area of the photodiode was open.

(ii) 4.5A: Only the area corresponding to the LED illumination on the shutter was open.

(iii) 10.78A: An area in between the LED illumination and PD surface area was open.

(iv) 54.85A: Entire shutter was open.

We plot the SNR versus different areas of shutter opening in Fig. 7. We report the minimum SNR over 10 trials for each area setting. We can observe from the SNR decreases significantly with increase in shutter opening area. This is in line with our theoretical understanding of the dependency of SNR on area of reception. In particular, if the receiver has a larger area of opening, it allows for more photons to be registered on the photodiode. However, if the desired signal occupies only a fraction of that area, the rest corresponds to accumulating noise and other undesired photons. Due to the additive nature of photon energy, separating signal from noise becomes extremely challenging if the SNR is low.

The SNR values suggest that, if it can be ensured that the receiver photodiode is collecting only the photons corresponding to the actual signal, then the effect of noise on the receiver becomes almost negligible. The improvement in SNR, as can be observed from these measurements, is such that when the area corresponding to the exact photodiode area is opened while other parts of the shutter are closed, the SNR is at 17dB, compared to the -1dB SNR value when the entire shutter was open. The negative SNR indicates that the noise component over powered the signal and hence demodulation is impossible. We also observe that the area of reception corresponding to the LED (4.5A) is not necessarily the best choice. This is because, the LED signal when projected on the shutter, acts like a diffuse source. The optical energy from the LED is distributed over a larger area (than the photodiode), thus, relatively, allowing for more noise photons to be registered at the receiver.

It is also notable that 18dB increase in SNR can be considered dramatic in terms of communication systems and are usually achieved only through extremely sophisticated and complex signal processing. Our measurements suggest that it may be achieved through a rethinking of the receiver hardware.

Setup	V_r	V_I	V_n	$SINR[dB]$
Openbox+Shutter open	5.0	3.7	0.7	-1.18
Openbox+Shutter (I+N) closed	4.1	0	0.7	15.22
Closedbox+Shutter open	4.9	3.6	0.4	-0.81
Closedbox+Shutter (I+N) closed	4.2	0	0.2	26.43

TABLE I: SINR measurements in open box and closed box setups when all optical sources are in always-ON (DC) mode. All voltage values are in Volts. Shutter (I+N) closed means the pixels corresponding to interference and noise projections on the shutter were closed. The closed box setup was not a totally dark setup. There is slight ambient light entry which was measured and calibrated to be 0.2V.

VI. Spatial Interference Cancellation

We conducted an interference and noise cancellation measurement experiment using the openbox and closedbox setups shown in Fig. 6. We treat the RED LED as light source, another RED LED as interfering source and the RED LASER as noise source. The ambient lighting in the room (white light from ceiling) is accounted as an additional noise source. We conducted measurements of received signal voltage V_r, noise voltage V_n and interference voltage V_I across open box and closed box setups, and along two modes of area selection: (i) Shutter fully open, (ii) Only pixels corresponding to noise LED and interference LASER LED projections were closed. During these measurements, all the light sources were input with a constant power and were set to operate in their maximum optical power output (supply maximum forward current). We compute the $SINR$ using the voltage measurements as,

$$SINR = \frac{V_r^2 - (V_I^2 + V_n^2)}{V_I^2 + V_n^2} \tag{2}$$

We report our measurements and SINR values in TABLE I.

We can observe from TABLE I that when the shutter is fully open or when the interference area was closed, the signal power almost remained constant. However, the interference can significantly overpower the signal if it were allowed to register on the photodiode. We can observe that the laser source which has a significantly higher optical power than the LEDs can completely overpower the system and hence lead to SINRs that are almost useless (close to zero or negatives). We also can observe that, even with an overpowering interfering source, through spatial filtering, the SINR can be dramatically improved, in ranges of 15-25dB.

In the next set of experiments, we set up to modulate the LEDs using a single frequency pulse waveform. We connected the signal and noise LEDs to the GPIO pins of RaspberryPi . We modulated each LED using a separate Raspberry Pi, which was controlled using MATLAB on a laptop. The waveform input to the LED was generated in MATLAB and communicated to the LED via the RaspberryPi. The signal LED was modulated at 300Hz (the pulse waveform read as 295Hz due to some distortions in the RaspberryPi link) with a 8V peak-peak pulse waveform. The noise LED was input with a 3V peak-peak pulse waveform at 100Hz. The laser LED was set in DC mode.

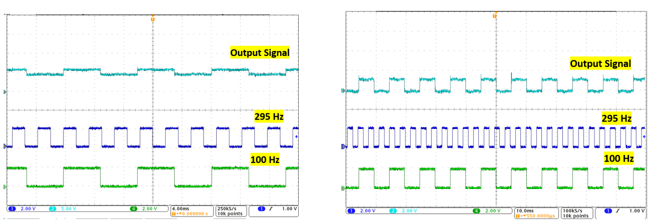

(a) Open shutter (b) Closed shutter

Fig. 8: Illustrating additive interference from alternating (AC) signals on the photodiode receiver. The measurement was taken with the shutter opened and shutter closed in closed box setup.

We can observe the additive property of optical signals in Fig. 8 . We can observe that the two signals plus the DC noise (laser beam) is added in the output. When signals of the same frequency are accumulated on the phototodiode, due to a phase difference of 0 (or 2π), the resultant signal is essentially an amplified version of the original signals.

When the phase difference is non–zero (or not 2π), then the effective phase–shift will be captured in the additive signal on the photodiode output. Assuming, we know atleast one of the transmit frequencies, through a cross correlation mechanism we can find out the phase difference and hence differentiate the waveforms at the receiver. However, the temporal separation of the waveform will be possible only when the receiver can ensure that it is exactly sampling the signals and not any unwanted optical energy. Also it requires knowledge of atleast one of the frequencies in the set. Hence, resolving the signal from noise from this cumulative signal is extremely challenging without calibrating the noise and interference levels, which adds complexity and usability constraints on the VLC system.

VII. Conclusion and Future Work

In this paper, we presented a new architecture that combines the high–speed sampling advantage of photodiodes with the spatial filtering capability of image sensor receivers. We presented a hybrid architecture design that uses a high–speed photodetector and an LCD shutter acting as a programmable image sensor aperture. We conducted measurements to study noise and interference separability in our receiver. Our measurements indicate that the spatial separability, if achieved correctly, can help improve the signal quality in the receiver and almost completely eliminate noise. Additionally, our measurements reveal that it is possible, invoking simple fundamental receiver techniques, to demodulate an optical pulse waveform if there is clear knowledge that the detected signal is clean, devoid of any interference. The hybrid receiver presents a clear opportunity to invoke simpler receiver techniques through smart spatial filtering mechanisms.

In this paper, the notion of the prototype implementation was to show a proof–of–concept understanding. Through the knowledge gained from the measurements using this setup, in future, we will design a custom receiver that leverages the advantages claimed by the design. In our future work, we will develop fast spatial tracking mechanisms for identifying the location of the signal on the shutter and design spatial tracking mechanisms under mobility. We believe that this paper essentially sets a foundation step towards ultra–high–speed VLC designs for the near future.

VIII. Acknowledgments

This work has been supported by the CISE CRII Program of the National Science Foundation under the grant NSF CRII CNS-NeTS 1755925. We would also like to thank the anonymous reviewers for their valuable comments and suggestions that has helped us improve the quality of this paper.

References

[1] T. Komine and M. Nakagawa. Fundamental analysis for visible-light communication system using led lights. *IEEE Transactions on Consumer Electronics,*, 50(1):100–107, Feb 2004.

[2] Visible light communication consortium. http://vlcc.net.

[3] Augmented reality using vlc. http://visiblelightcomm.com/augmented-reality-using-vlc/.

[4] Philips indoor vlc positioning technology. http://www.lighting.philips.com/main/systems/themes/led-based-indoor-positioning.

[5] Haruyama T.Saito and Nakagawa. Inter-vehicle communication and ranging method using led rear lights. *Proceedings of the fifth IASTED international conference on Communication Systems and Networks*, 5:278–283, Aug 2006.

[6] Firefly underwater vlc. http://www.fireflywirelessnetworks.com/underwater-applications.html.

[7] A. Ashok. Doctoral dissertation: Design, modeling and analysis of visual mimo communication. In *RUcore: Rutgers University Community Repository*, 2014. NJ, USA.

[8] Ieee 802.15.7 wpan task group 7: Visible light communication. http://www.ieee802.org/15/pub/TG7.html.

[9] purelifi: The lifi technology. http://purelifi.com/.

[10] Why the internet pipes will burst when virtual reality takes off. https://www.forbes.com/sites/valleyvoices/2016/02/09/why-the-internet-pipes-will-burst-if-virtual-reality-takes-off/#45e0ad303858.

[11] Wigig (60ghz wireless communication) alliance. http://www.wi-fi.org/discover-wi-fi/wi-fi-certified-wigig.
[12] Ieee 802.15.7r1 status, 2015. http://vlca.net/site/wp/wp-content/uploads/2016/01/2015_10_26_YeongMinJangICEVLC2015CC.pdf.
[13] A. Goldsmith. *Wireless Communications*. Cambridge University Press, 2005.
[14] S. Rajbhandari, A. V. N. Jalajakumari, H. Chun, G. Faulkner, K. Cameron, D. Tsonev, H. Haas, E. Xie, J. J. D. McKendry, J. J. D. Herrnsdorf, R. Ferreira, E. Gu, M. D. Dawson, and D. C. O'Brien. A multi-gigabit/sec integrated multiple input multiple output vlc demonstrator. *Journal of Lightwave Technology*, PP(99):1–1, 2017.
[15] Sonys 1000fps camera. https://www.sony.net/SonyInfo/News/Press/201702/17-013E/index.html.
[16] A. T. Hussein and J. M. H. Elmirghani. 10 gbps mobile visible light communication system employing angle diversity, imaging receivers, and relay nodes. *IEEE/OSA Journal of Optical Communications and Networking*, 7(8):718–735, August 2015.
[17] Avalanche photodiodes. https://www.edmundoptics.com/testing-detection/detectors/avalanche-photodiodes/.
[18] S. Perli, N. Ahmed, and D. Katabi. Pixnet: Lcd-camera pairs as communication links. In *SIGCOMM*, pages 451–452, 2010.
[19] Tian Hao, Ruogu Zhou, and Guoliang Xing. Cobra: Color barcode streaming for smartphone systems. In *Proceedings of the 10th International Conference on Mobile Systems, Applications, and Services*, MobiSys '12, pages 85–98, New York, NY, USA, 2012. ACM.
[20] Tianxing Li, Chuankai An, Xinran Xiao, Andrew T. Campbell, and Xia Zhou. Real-time screen-camera communication behind any scene. In *Proceedings of the 13th Annual International Conference on Mobile Systems, Applications, and Services*, MobiSys '15, pages 197–211, New York, NY, USA, 2015. ACM.
[21] Anran Wang, Zhuoran Li, Chunyi Peng, Guobin Shen, Gan Fang, and Bing Zeng. Inframe++: Achieve simultaneous screen-human viewing and hidden screen-camera communication. In *Proceedings of the 13th Annual International Conference on Mobile Systems, Applications, and Services*, MobiSys '15, pages 181–195, New York, NY, USA, 2015. ACM.
[22] Robert LiKamWa, David Ramirez, and Jason Holloway. Styrofoam: A tightly packed coding scheme for camera-based visible light communication. In *Proceedings of the 1st ACM MobiCom Workshop on Visible Light Communication Systems*, VLCS '14, pages 27–32, New York, NY, USA, 2014. ACM.
[23] Wenjun Hu, Hao Gu, and Qifan Pu. Lightsync: Unsynchronized visual communication over screen-camera links. In *Proceedings of the 19th Annual International Conference on Mobile Computing & Networking*, MobiCom '13, pages 15–26, New York, NY, USA, 2013. ACM.
[24] Wenjun Hu, Jingshu Mao, Zihui Huang, Yiqing Xue, Junfeng She, Kaigui Bian, and Guobin Shen. Strata: Layered coding for scalable visual communication. In *Proceedings of the 20th Annual International Conference on Mobile Computing and Networking*, MobiCom '14, pages 79–90, New York, NY, USA, 2014. ACM.
[25] Smart lighting research center. http://www.bu.edu/smartlighting/.
[26] N. O. Tippenhauer, D. Giustiniano, and S. Mangold. Toys communicating with leds: Enabling toy cars interaction. In *2012 IEEE Consumer Communications and Networking Conference (CCNC)*, pages 48–49, Jan 2012.
[27] H. Ma, L. Lampe, and S. Hranilovic. Integration of indoor visible light and power line communication systems. In *2013 IEEE 17th International Symposium on Power Line Communications and Its Applications*, pages 291–296, March 2013.
[28] Jiangtao Li, Angli Liu, Guobin Shen, Liqun Li, Chao Sun, and Feng Zhao. Retro-vlc: Enabling battery-free duplex visible light communication for mobile and iot applications. In *Proceedings of the 16th International Workshop on Mobile Computing Systems and Applications*, HotMobile '15, pages 21–26, New York, NY, USA, 2015. ACM.
[29] Junrui Yang Chenren Xu Guobin Shen Guojun Chen Xieyang Xu, Yang Shen and Yunzhe Ni. Passivevlc: Enabling practical visible light backscatter communication for battery-free iot applications. In *Proc. ACM Mobile Computing and Networking (MobiCom)*, Oct 2017.
[30] P. H. Pathak, X. Feng, P. Hu, and P. Mohapatra. Visible light communication, networking, and sensing: A survey, potential and challenges. *IEEE Communications Surveys Tutorials*, 17(4):2047–2077, Fourthquarter 2015.
[31] A. Jovicic, J. Li, and T. Richardson. Visible light communication: opportunities, challenges and the path to market. *IEEE Communications Magazine*, 51(12):26–32, December 2013.
[32] Lcd shutters from liquid crystal technologies. http://www.liquidcrystaltechnologies.com/products/LCDShutters.htm.
[33] Ettus research: Usrp. https://www.ettus.com/.
[34] Sfh 206 k photodiodes. https://media.osram.info/media/resource/hires/osram-dam-2496052/SFH2020620K.pdf.
[35] Arduino. https://www.arduino.cc/.
[36] Red led ltl2r3ew3ks. https://media.digikey.com/pdf/Data%20Sheets/Lite-On%20PDFs/LTL2R3EW3KS_4-18-12.pdf.
[37] Wireless laser pointer. http://en.norwii.com/products/wireless-presenters/n36-wireless-presenter-with-laser-pointer/.
[38] Lcd shutters from 4d systems. https://www.4dsystems.com.au/product/uLCD_32PTU/.
[39] 2231a-30-3 triple channel dc power supply. http://www.farnell.com/datasheets/1851614.pdf?_ga=2.86734552.1915376789.1537558757-2036209346.1537558757.
[40] Mdo4000c mixed domain oscilloscope. https://www.tek.com/datasheet/mixed-domain-oscilloscopes-0.
[41] Camera module v2 from raspberrypi.org. https://www.raspberrypi.org/products/camera-module-v2/.
[42] Lm358 n dual operational amplifier. http://www.ti.com/lit/ds/symlink/lm358-n.pdf.
[43] Aspheric condenser lens. https://www.edmundoptics.com/p/27mm-diameter-x-13mm-fl-aspheric-condenser-lens/5446/.